UDC 622.831: 622,2: 622.235

V. A. EREMENKO[1], *Professor, Doctor of Engineering Sciences, prof.eremenko@gmail.com*
A. A. BRAGIN[2], *Development Director, Candidate of Engineering Sciences*
D. Yu. GRIDIN[2], *Presale–Engineer*
A. A. BYKOVA[3], *Senior Lecturer*

[1]*NUST MISIS' College of Mining, Moscow, Russia*
[2]*PRIN JSC, Moscow, Russia*
[3]*Peoples' Friendship University of Russia named after Patrice Lumumba, Moscow, Russia*

LASER SCANNING-BASED TRUE CONDITION OF MINE SHAFT

The article presents SLAM CHCNAV RS10 scanner data obtained in 2025 in an operating mine shaft. The list and execution speed of operations are reported, and the data interpretation is given. The processing order of the point cloud and the condition analysis of the test mine shaft are described. It is for the first time found that laser scanning determines many required parameters and characteristics which ensure safety, efficiency and facilitation of mining operations, namely: true condition and serviceability of operating mine openings; damage spots in support and lining, including visually unobservable areas; solid mineral output capacity both in open pit and underground mining; parameters of support and reinforcement in mine openings; rock mass stability, alignment of stopes and pillars; excessive volume of rock haulage per 1 m of stoping in case of increased design section of stopes, etc. Laser scanning with SLAM CHCNAV RS10 simplifies survey measurements and enhances efficiency of deformation monitoring. Periodic scanning of stopes exhibits deformation trends, high stress–strain areas in support and reinforcement system of stopes, as well as potential damage spots in support systems.

Keywords: *Shaft, SLAM CHCNAV RS10 scanner, point cloud, deformation, displacement, section, focal and shorter axes of elliptical shaft section, tubing support, cage*
DOI: *10.17580/em.2025.01.09*

Introduction

Modern technologies of scanning in mines [1–4], including long and deep underground openings [5–7], enjoy high demand at the present-day phase of development of mining in the 21st century. This article describes the analytical data on deformation of a cage shaft in an operating mine, with detection of the most abnormal sites, and presents recommendation on visual estimate of condition of mine shafts and on control of displacements in exposed areas.

The study aimed to assess the actual condition of a mine shaft to understand its further reconstruction and operation options [8–11]. The shaft scanning was carried out by 2 workers for 2 days, and the data were processed and interpreted within 2 weeks. SLAM CHCNAV RS10 scanner was arranged under the cage floor, at the bottom of the inspection window (**Fig. 1**). It was decided to be inexpedient to set the scanner above the cage because of water entry in the shaft and owing to periodic rock falls.

Fig. 1. Arrangement of SLAM CHCNAV RS10 scanner beneath the cage

The scope of work included:

- Laser scanning of the shaft using SLAM CHCNAV RS10 scanner (**Fig. 2**) [12–15];
- Building of the actual frame of the shaft in Micromine (or another similar program) using the obtained cloud of points;
- Plotting of a regular vertical shape of a round project shaft frame with the diameter of 4.5 m and a regular non-vertical shape of a round shaft with the diameter of 4.5 m with regard to the actual inclinations of shafts as per in-mine records;
- Measurement of actual deviations in the operating non-regular shape shaft from the regular non-vertical roundness 4.5 m in diameter with regard to actual inclinations in 8 directions (north, south, west, east, northwest, northeast, southwest and southeast) and, selectively, on the sites of abnormal deviations (difference between the long focal and shorter axes of the cross-section ellipse of the shaft) from the regular roundness 4.5 m in diameter;
- Analysis and processing of the data on deformations in the shaft;
- Comparison with the archive data on the shaft condition as of 1958;
- Assessment of actual condition and operational capacity of the shaft;
- Recommendations on possible optimization of the shaft performance [16–18].

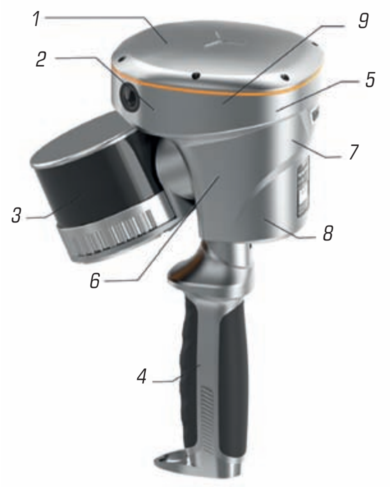

Fig. 2. SLAM CHCNAV RS10 scanner:
1 – scanner-integrated high-precision RTK (Real Time Kinematic); *2* – VIS (Visual Inertial System); *3* – cameras HD (High Definition); *3* – SLAM (Simultaneous Localization and Mapping), lidar has 16 or 32 channels; *4* – detachable handle to allow atop arrangement of the scanner; *5* – built-in IMU (Inertial Measurements Unit), frequency of 200 Hz; *6* – IP64 protection to operate in difficult conditions; *7* – memory 500 Gb or 1 Tb in capacity; *8* – fast-replaceable battery capable to operate up to 60 min; *9* – powerful computer for processing SLAM data and point cloud coloring in real time. Picture is courtesy of PRIN JSC

Processing of cloud of shaft points

Processing of the point cloud obtained using GNSS–RTK-based SLAM CHCNAV RS10 scanner [19] was carried out in Micromine.

The scope of these works included:

1. Import of the point cloud in Micromine;

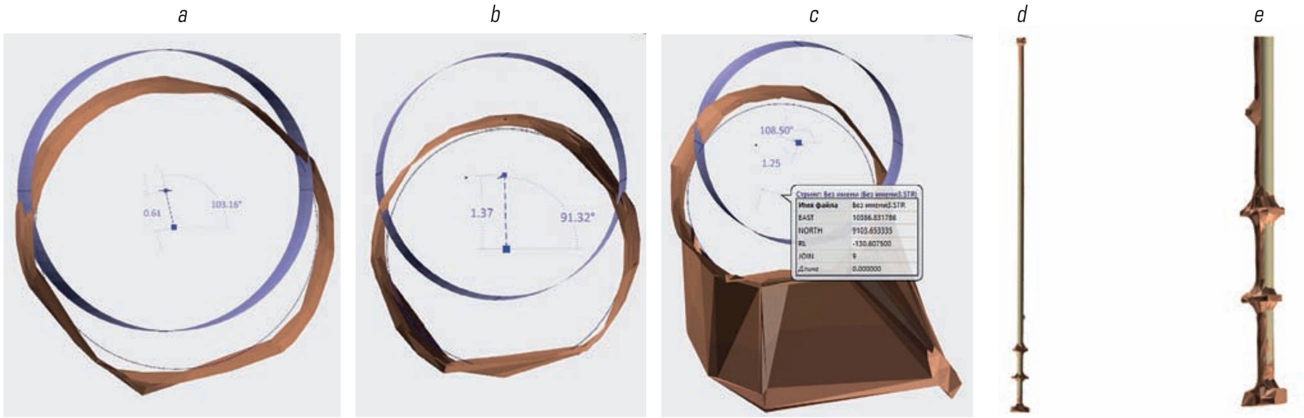

Fig. 3. True shaft frame from point cloud versus vertical roundness 4.5 m in diameter with inclination disregarded, elevation +35.197 m, disagreement 0.61 m (*a*); elevation –37.705 m, disagreement 1.37 m (*b*); elevation –130.608 m, disagreement 1.25 m (*c*). Collation of true shaft frame and its segments with vertical roundness 4.5 m in diameter with regard to inclination: (*d*) northward view; (*e*) eastward view

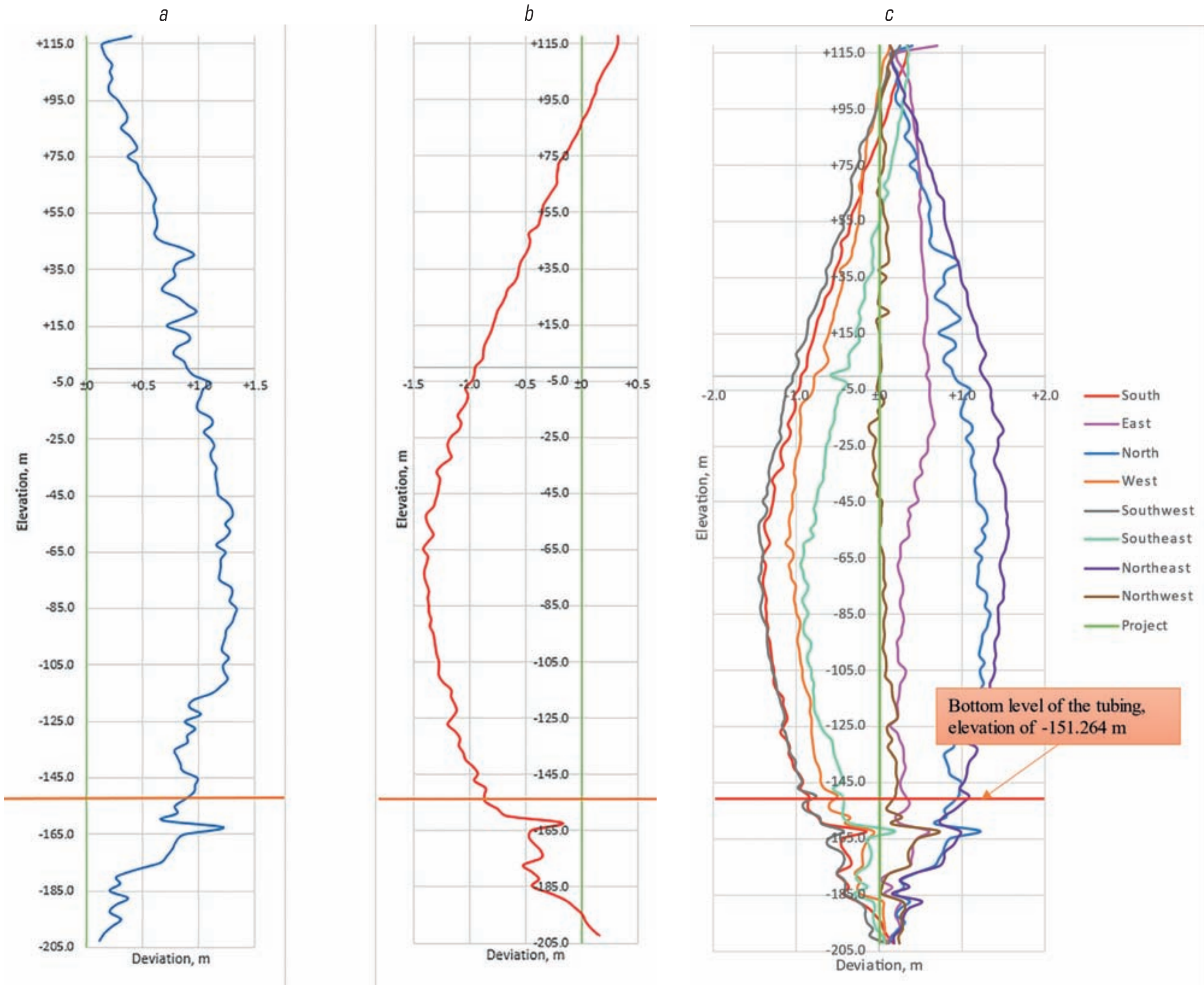

Fig. 4. Disagreement in the line of the North (*a*) and South (*b*). General disagreement pattern along the shaft (*c*)

2. Creation of the external shaft shell (frame) using the point cloud (**Fig. 3**);
3. Construction of the project shaft frame of a regular vertical round cross-section shape with the diameter of 4.5 without regard to the actual recorded inclination;
4. Construction of the project shaft frame of a regular vertical round cross-section shape with the diameter of 4.5 with regard to the actual recorded inclination. The inclination appeared supposedly in shaft sinking initially along a non-vertical trajectory;

5. Comparison of the shaft frame from the point cloud with the regular vertical project shaft frame 4.5 m in diameter with regard to the actual recorded inclination. At this stage, the actual deviation of the shaft from the vertical is determined using two proposed methods;

6. Plotting of the shaft section every 2.5 m from the surface, starting from its actual elevation, with a view to estimate deformations;

7. In each section of the actual external frame of the shaft, estimation of its geometrics, measurement of displacements of the actual shaft frame from the point cloud relative to the regular vertical roundness of the shaft frame 4.5 m in diameter with regard to the actual recorded inclination in 8 directions: north, south, west, eats, northwest, northeast, southwest and southeast;

8. Selectively, at the points of the abnormal deviations from the regular roundness 4.5 m in diameter (difference between the lengths of the focal and shorter axes of the shaft cross-section ellipse), analysis and, if necessary, visual assessment of damage in the shaft support or adjacent rock mass;

9. Plotting and analysis of deformation curves by the points of the shaft cross-section in Microsoft Excel.

Studies on the actual condition of the shaft

Deviations of the shaft from the vertical axis were studied by two methods: 1) using a plumb line (the method adopted at the test mine) and 2) comparison of the direction of the ideal vertical axis and the existing deviation of the shaft axis.

In the comparison of the actual shaft frame from the point cloud with the regular vertical shape of the project shaft frame with the diameter of 4.5 m without regard to the actual inclination, the deviation of the shaft from the vertical axis is recorded in the north and northwest directions by 0.41 and 0.96 m, respectively (**Table**).

Table. Measured inclinations of the shaft from the vertical axis

Actual elevation, m	North, m	Northwest, m	South, m	Southeast, m
+1	2.52	2.54	2.45	2.42
–129.563	3.42	3.32	1.00	1.05
–134.7	3.13	3.49	1.03	1.05
–171.6	2.82	3.66	1.50	1.17
–194.9	2.34	3.51	1.58	1.16

In the comparison of the actual shaft frame from the point cloud with the regular vertical shape of the project shaft frame with the diameter of 4.5 m without regard to the actual inclination, the deviation of the shaft from the vertical axis in the northwest direction is 1.37 m at the elevation of –37.705 and 1.25 m at the elevation of –130.608 m, supposedly, owing to the shaft sinking along initially a non-vertical trajectory (see Figs. 3*a*, 3*b* and 3*c*).

In the comparison of the actual shaft frame with the regular vertical roundness 4.5 m in diameter (see Figs. 3*d* and 3*e*), with regard to the actual inclination, the deviations measured in the selected directions are shown individually and in the general diagram in **Fig. 4**. The deviation with a minus sign means the displacement inward the shaft; the deviation with a plus sign means the displacement toward the adjacent rock mass. The deviations in Fig. 4 are given in meters.

The orange color line in Fig. 4 marks the lower level of the tubing column.

At the points of abnormal deviations from the regular shaft roundness with the diameter of 4.5 m (the length difference between the focal and shorter axes of the shaft cross-section ellipse), the shape transformations were analyzed. The selected results are shown in **Figs. 5*a*** and **5*b*** (the spatial orientation of the cross-sections is demonstrated in **Fig. 5*c***).

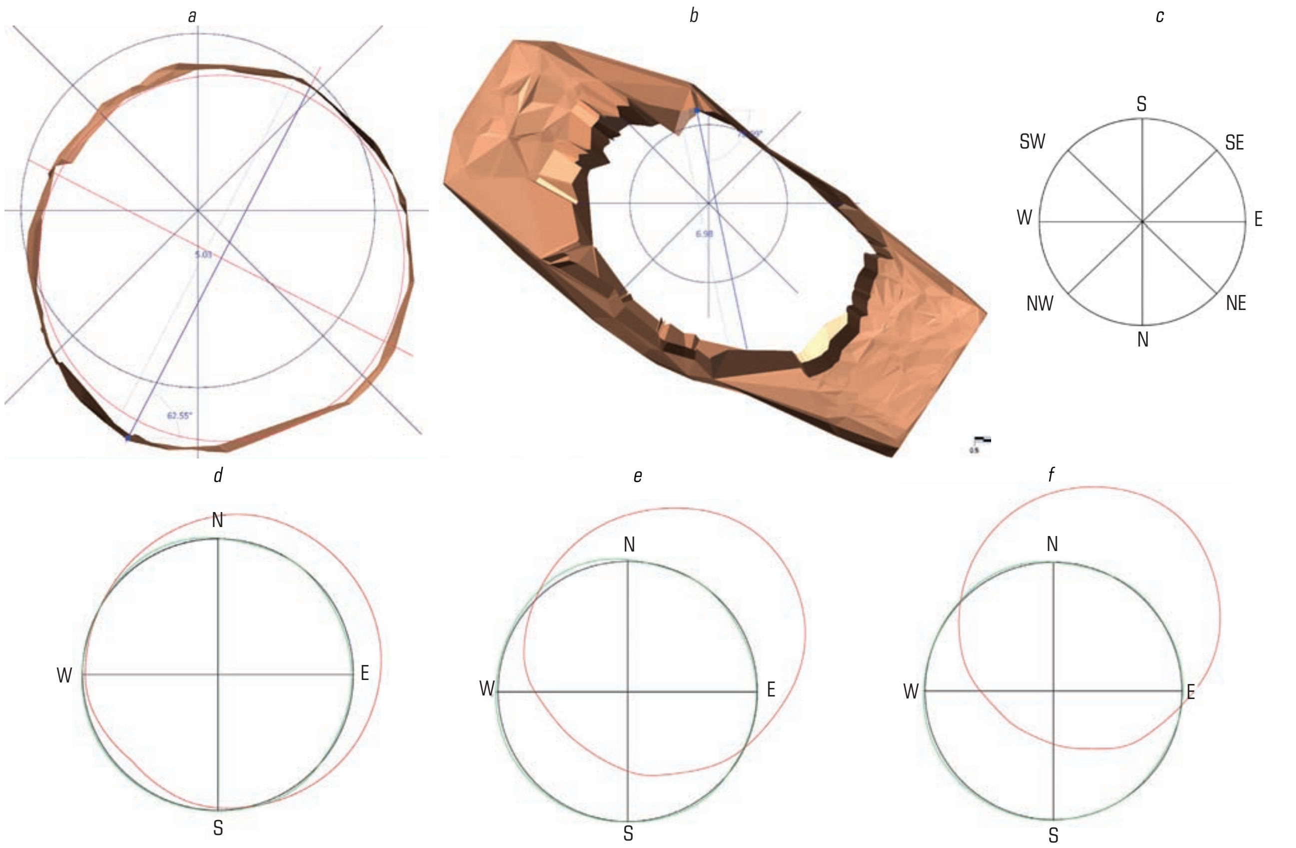

Fig. 5. Shaft section at elevation of –169.96 m (focal axis length 5.03 m (horizontal angle), shorter axis length 4.79 m) (*a*) and at elevation -182.46 m (shaft station) (*b*). Spatial orientation of sections (*c*). Deformation trend in the shaft in 1958–2024 at elevations +82.54 m (*d*), +7.54 m (*e*) and –97.46 m (*f*)

Fig. 6. Fracture in cast-iron tubing (level 88–89 in the shaft) and horizontal section at level 88 at elevation –145.275 m

The horizontal section of the vertical roundness shaft with the diameter of 4.5 m with regard to the inclination is marked with the grey color circle, and the actual frame of the shaft is colored in orange.

Starting from ground surface, a gradual increase is recorded in deviations toward the mid-depth of the shaft, with their gradual decrease toward the bottom at the level of –212.46 m. In the south and southwest directions, the highest minus-sign deviations are recorded at the levels of –4.96 to –132.46 m: –1.42 and –1.46 m, respectively. In the north and northeast directions, the maximal plus-sign deviations are recorded at the levels of +20.04 to –134.96 m: +1.34 and +1.55 m, respectively.

The trends of deformation directions in the shaft are determined at the shaft top, middle and bottom (**Figs. 5*d*, 5e and 5*f***).

Along the whole shaft, abridgment is recorded in the northwest part of the shaft, which is connected with the presence of the stairways.

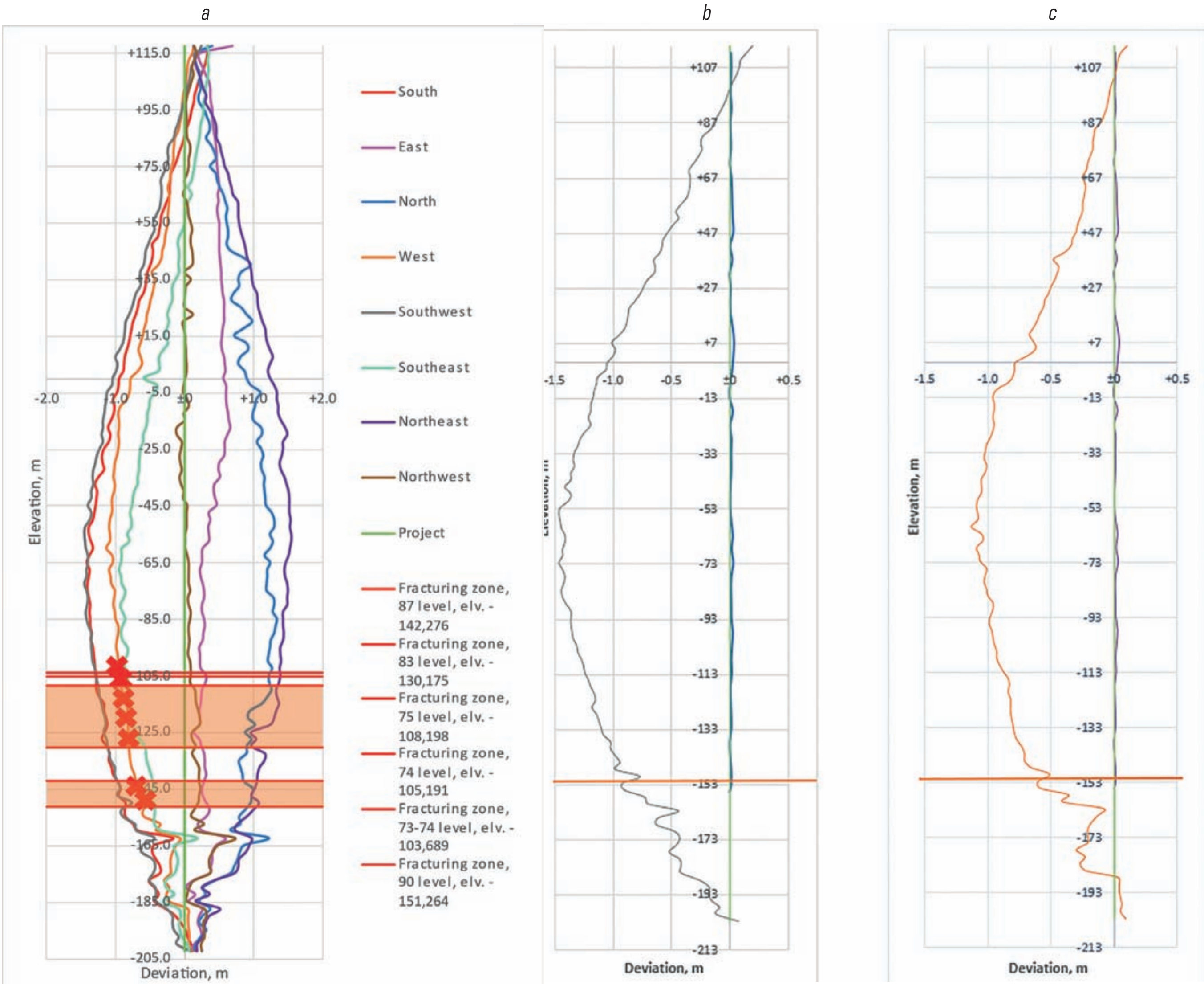

Fig. 7. Total deformation pattern in the shaft with regard to recorded and anticipated fractures in tubing (*a*). Profiles South–West (horizontal angle 21.46) (*b*) and West (horizontal angle 23.54) (*c*) (curves at vertical axis, data as of 1958; large drift curves, data as of 2025)

At the levels of –132, –160, –168, –185 and –215 m in the shaft, a substantial increase in the plus-sign deviations is recorded in all directions, associated with the shaft stations; the data on these levels are withdrawn from the analysis as they are incorrect.

At the levels of –100.46, –105.191, –108.54 to –130.174 and –142.276 to –151.264 m in the west wall of the shaft, cracks are recorded in the tubing and fracturing zones are predicted (**Figs. 6** and **7*a***).

The current condition of the shaft is compared with its condition as per Act 1958 (**Figs. 5*d***, **5*e***, **5*f***, **7*b*** and **7*c***).

From the implemented research, it is found that:

1. The tubing support breaks in the sites intersected by the focal or by the shorter axes of the shaft cross-section ellipse due to the change in the physical and mechanical properties of the tubing material because of the metal corrosion and ageing for over 60 years. The tensile cracks at the intersections by the shorter axes are visually seen, while the tensile cracks at the intersections with the focal axis are visually unseen as they appear on the back side of the lining.

2. In the unsupported areas in the shaft, adjacent rock mass experiences maximal displacements inside the shaft, along the shorter axes; at the intersections by the focal axis, rock mass undergoes intense deformation (fracturing induced by the action of rock pressure);

3. The length difference between the focal and shorter axes are the limit displacements (these data are required for the support design in the periods of the shaft construction, repair or reconstruction);

4. The periodic monitoring of the shaft using SLAM-scanning data allow defining the shaft deformation trends (directions of maximal deformations, stress–strain areas in support, potential damage and failure areas in support, etc.);

5. The data of SLAM-scanning allow determination of action paths of the principal horizontal and sub-horizontal stresses in rock mass.

Conclusions

The GNSS–RTK-based SLAM CHCNAV RS10 scanning of mine shafts simplifies surveying and effective monitoring of initiation of deformation processes.

Periodic scanning of mine shafts enables detecting the shaft deformation trends, the hazardous stress–strain sites in the shaft support, and the potential damage areas in the shaft lining.

In unsupported areas of mine shafts, rocks maximally displace inside the shafts along the shorter axis the shaft cross-section ellipse; at intersections of the focal axis and the shaft boundary, rock mass violently deforms (rock pressure-induced fracturing).

Shaft support breaks at intersections of the focal or shorter axes with the shaft boundary.

The length differences between the focal and shorter axes are the limit displacement in rock mass (these data are required for the support design in the time of construction, repair or reconstruction of mine shafts).

Scanning in mines makes it possible to: control the process of solid mineral extraction in both open pit and underground mining; design support and reinforcement systems for mine openings; determine rock mass stability categories, as well as actual condition and operability of mine openings; if necessary, align mine openings in case of the room-and-pillar mining method; record extra volume of rocks per 1 of borehole in case of outbreaks in case of drilling and blasting, etc.

For scanning access/development/breakage headings, mined-out voids and open pits using the GNSS–RTK-based SLAM CHCNAV RS10 scanner, and for the interpretation of the obtained data, a team of technical experts from PRIN and researchers from the Center for Applied Geomechanics and Convergent Technologies in Mining, NUST MISIS' College of Mining has been gathered.

References

1. Dmitriyev S. V. Development of tools for volumetric scanning and profiling of underground working. *Vestnik Nauchnogo Centra RAN*. 2021. Vol. 13, No. 3. pp. 22–27.
2. Valkov V. A., Valkova E. O., Mustafin M. G. Methodology for refining digital relief models of open-pit mine workings based on laser scanning and aerial photography. *Mine surveying and subsurface use*. 2023. No. 3(125). pp. 40–52.
3. Vystrchil M. G., Mukminova D. Z., Baltyzhakova T. I., Paramonov V. G., Valkova E. O. Analysis of deformation processes by survey data of laser scanning and photogrammetry. *MIAB*. 2025. No. 2. pp. 78–98.
4. Okhotin A. L., Belyaev E. N. Mobile laser scanning of underground mine openings using inertial navigation systems. *Mine Surveying Bulletin*. 2011. No. 6(86). pp. 31–34.
5. Tarasov V. V., Aptukov V. N. Laser scanning monitoring of deformations in concrete lining of mine shafts. *Fiziko-texhnicheskiye problemy razrabbotki poleznykh iskopaemykh*. 2022. No. 5. pp. 188–195.
6. Pleshko M. S., Pankratenko A. N., Pleshko M. V., Nasonov A. A. Assessment of stress–strain behavior of shaft lining in bottomhole area during sinking by real-time monitoring and computer modeling data. *Eurasian mining*. 2021. No. 1. pp. 25–30.
7. Pleshko M. S., Golembo O. D. Methodology for determining the parameters of shotcrete fastening mine shafts passed through the drilling method. *Izvestiya TulGU. Nauki o Zemle*. 2024. No. 2. pp. 403–415.
8. Stupnik N. I., Popov S. O., Azaryan V. A., Karamanits F. I. Research of parameters of development of deformation processes in underground excavations, using an automated laser scanning systems. *Gornyi Zhurnal*. 2014. No. 5. pp. 70–73.
9. Druz R. A., Protasova A. V., Asafiev I. A., Korytov A. S., Okhunov Sh. R. Comparison of calculated volumes of mine openings using tacheometer and ground-based laser scanning. *Geology, Prospecting and Exploration of Minerals and Geological Research Methods: International Conference Proceedings*. 2022. Iss. 22. pp. 202–204.
10. Rakhatkulov D. Kh., Zainitdinova R. M. Modeling mine roadways using laser scanning. *Nauchnye Issledovaniya i Razrabotki Molodykh Uchenykh*. 2016. No. 9-1. pp. 148–152.
11. Melnikov V. G., Grigorov A. M. Method for automated surface diagnostics of technical condition of underground miningworkings. Patent RF, No. 2810350. Applied: 27.07.2023. Published: 27.12.2023.Bulletin No. 36.
12. Wang Y., Song W., Lou Y. et al. Rail vehicle localization and mapping with LiDAR-vision-inertial-GNSS fusion. *IEEE Robotics and Automation Letters*. 2022. Vol. 7, Iss. 4. pp. 9818–9825.
13. Wang Y., Lou Y., Song W., Tu Z. A tightly-coupled framework for large-scale map construction with multiple non-repetitive scanning LiDARs. *IEEE Sensors Journal*. 2022. Vol. 22, Iss. 4. pp. 3626–3636.
14. Wang Y., Lou Y., Zhang Y. et al. A robust framework for simultaneous localization and mapping with multiple non-repetitive scanning lidars. *Remote Sensing*. 2021. Vol.13, Iss. 10. ID 2015.
15. Wang Y., Lou Y., Song W., Tu Z., Zhang S. Simultaneous localization of rail vehicles and mapping of surroundings with LiDAR-inertial-GNSS integration. *IEEE Sensors Journal*. 2021. Vol. 22, Iss. 14. pp. 14501–14512.
16. Sidorov D. V., Ponomarenko T. V. Estimation methodology for geodynamic behavior of nature-and-technology systems in implementation of mineral mining projects. *Gornyi Zhurnal*. 2020. No. 1. pp. 49–52.
17. Eremenko V. A., Ainbinder I. I., Marysyuk V. P., Nagovitsyn Yu. N. Guidelines for selecting ground support system for the Talnakh operations based on the rock mass quality assessment. *Gornyi Zhurnal*. 2018. No. 10. pp. 101–106.
18. Louchnikov V. N., Eremenko V. A., Sandy M. P., Kosyreva M. A. Rock Bolting Design for Mines Exposed to Rockburst Hazard. Journal of Mining Science. 2017. Vol. 53, Iss. 3. pp. 504–512.
19. Dai X., Song W., Wang Y. et al. Lidar–inertial integration for rail vehicle localization and mapping in tunnels. *IEEE Sensors Journal*. 2023. Vol. 23, Iss. 15. pp. 17426–17438. EM